

# Geophysical constraints on the dynamics of spreading centres from rifting episodes on land

Tim J. Wright<sup>1\*</sup>, Freysteinn Sigmundsson<sup>2</sup>, Carolina Pagli<sup>1</sup>, Manahloh Belachew<sup>3</sup>, Ian J. Hamling<sup>4</sup>, Bryndís Brandsdóttir<sup>2</sup>, Derek Keir<sup>5</sup>, Rikke Pedersen<sup>2</sup>, Atalay Ayele<sup>6</sup>, Cindy Ebinger<sup>3</sup>, Páll Einarsson<sup>2</sup>, Elias Lewi<sup>6</sup> and Eric Calais<sup>7</sup>

**Most of the Earth's crust is created along 60,000 km of mid-ocean ridge system. Here, tectonic plates spread apart and, in doing so, gradually build up stress. This stress is released during rifting episodes, when bursts of magmatic activity lead to the injection of vertical sheets of magma — termed dykes — into the crust. Only 2% of the global mid-ocean ridge system is above sea level, so making direct observations of the rifting process is difficult. However, geodetic and seismic observations exist from spreading centres in Afar (East Africa) and Iceland that are exposed at the land surface. Rifting episodes are rare, but the few that have been well observed at these sites have operated with remarkably similar mechanisms. Specifically, magma is supplied to the crust in an intermittent manner, and is stored at multiple positions and depths. It then laterally intrudes in dykes within the brittle upper crust. Depending on the availability of magma, multiple magma centres can interact during one rifting episode. If we are to forecast large eruptions at spreading centres, rifting-cycle models will need to fully incorporate realistic crust and mantle properties, as well as the dynamic transport of magma.**

Less than 2% of Earth's mid-ocean ridge system is located above sea level. Although marine geophysical methods are very well suited for imaging the structure of mid-ocean ridges<sup>1,2</sup> and locating melt within the crust<sup>3</sup>, it is difficult to resolve active processes at submarine ridges. More commonly, inferences are made about dynamics of ridges by analogy with structures on land<sup>4</sup>, or from observations of crustal structures that seem to be transient<sup>5</sup>. Studies of magma transport at subaerial volcanoes have demonstrated the use of crustal deformation<sup>6,7</sup> and seismological<sup>8,9</sup> data for unravelling magma movements and magmatic plumbing systems. However, measuring both deformation and seismicity at submerged ridges during rifting is challenging, with only few examples where any data have been recovered<sup>10–14</sup>.

Here we review geophysical observations of dynamic rifting processes at the two subaerial portions of mid-ocean ridge in Iceland and the Afar region in Africa (Fig. 1), and also present several unpublished results. Iceland sits astride the mid-Atlantic ridge in the North Atlantic where plate spreading began about 60 million years ago. The full plate-spreading rate of  $\sim 19$  mm yr<sup>-1</sup> is accommodated within Iceland<sup>15,16</sup>. The Afar region forms an approximately triangular region at the northern end of the East African rift and contains the triple junction between the separating Nubian, Somalian and Arabian plates (Fig. 1). Spreading centres that are located beneath the Red Sea and Gulf of Aden jump on land in Afar, where rifting has proceeded from continental extension to nascent seafloor spreading over the past 30 million years<sup>17,18</sup>. Current rates of extension between Arabia and the two African plates are on the order of 16–20 mm yr<sup>-1</sup> (refs 19,20). Both Afar and Iceland have anomalously thick and elevated crust due to the enhanced melting and dynamic topography induced by mantle plumes<sup>21–25</sup>.

The ridge axes in both Iceland and Afar are divided into 60–100-km-long portions, known as magmatic segments in Afar<sup>26</sup> and volcanic systems in Iceland<sup>16</sup>. We use the term 'spreading centre' here to describe these segments/systems, as they are analogous to the second-order, non-transform offset segments observed on slow-spreading mid-ocean ridges<sup>27</sup>. In this Review, we give particular weight to observations from rifting episodes, three of which have occurred subaerially in the modern era. Seismic activity associated with these rifting episodes has been measured and can be used to identify the magmatic plumbing systems. Furthermore, magma movements result in diagnostic surface deformation that can be used to infer the processes involved in rifting episodes. We also review constraints on the properties of crust and mantle at spreading centres that can be obtained by examining the response to the major stress changes associated with the rifting episodes. Because the rifting deformation cycle takes  $\sim 10^2$ – $10^3$  years to complete, one must consider a range of different spreading centres to constrain the entire cycle. We discuss observations from the Askja spreading centre in Iceland to help constrain processes occurring between rifting episodes. Finally, we construct a conceptual model for spreading centres that satisfies observations from these different locations and time periods, and discuss the implications for mid-ocean ridges.

## Subaerial rifting episodes in the modern era

Our understanding of the mechanics of magmatic rifting has been transformed by observations of rifting episodes at subaerial spreading centres in Iceland (Krafla, 1975–1984) and Afar (Asal-Ghoubbet, 1978; Dabbahu, 2005–2010?). Here we summarize observations from these episodes, highlighting common features.

<sup>1</sup>COMET+ School of Earth and Environment, University of Leeds, Leeds LS2 9JT, UK, <sup>2</sup>Nordic Volcanological Centre, Institute of Earth Sciences, University of Iceland, Sturlugata 7, 101 Reykjavík, Iceland, <sup>3</sup>Department of Earth & Environmental Sciences, University of Rochester, Rochester, New York 14627, USA, <sup>4</sup>International Centre for Theoretical Physics, 11 Strada Costiera, Trieste I-34151, Italy, <sup>5</sup>National Oceanography Centre Southampton, University of Southampton, European Way, Southampton SO14 3ZH, UK, <sup>6</sup>Institute for Geophysics, Space Science and Astronomy, Addis Ababa University, Addis Ababa, Ethiopia, <sup>7</sup>Department of Earth and Atmospheric Sciences, Purdue University, West Lafayette, Indiana 47907-2051, USA.

\*e-mail: t.j.wright@leeds.ac.uk

From 1975 to 1984, around 20 dyke intrusions occurred in the Krafla spreading centre<sup>16,28</sup>, generating earthquake swarms<sup>29–31</sup>, surface faulting<sup>32</sup> and widening<sup>33,34</sup> (Figs 2 and 3). Cumulative widening averaged to 4–5 m, corresponding to 2–2.5 centuries of long-term spreading<sup>33</sup>. Each event was directly correlated with activity within the Krafla caldera, where subsidence occurred as the dyke propagated laterally away from the caldera at rates of 0.2–0.6 m s<sup>-1</sup> (ref. 29). Between dyking events, seismicity was mostly confined to the caldera (Fig. 3), which uplifted at a rate of up to 6 mm day<sup>-1</sup>, fastest immediately following a dyke intrusion and gradually slowing down<sup>35</sup> (Fig. 2e). A low seismic velocity anomaly and shear wave attenuation at 3–5 km depth has been interpreted as a shallow magma chamber<sup>36</sup>. It is located within a high velocity ‘chimney’ — probably a complex of intrusions — extending from the base of the crust. Magma has also been imaged seismically from S-wave shadows<sup>37</sup> and by reflection from the base of the shallow chamber<sup>38</sup>.

The initial dyke intrusion in December 1975 was by far the largest in the episode, intruding a ~60-km-long segment of the spreading centre<sup>29</sup>. Most widening occurred ~50 km north of the Krafla caldera, where seismicity was also most intense<sup>28</sup> (Figs 2d and 3e). The dyke was associated with a minor eruption within the Krafla caldera, which subsided by up to 2 m, consistent with a pressure drop in the shallow magma chamber. The initial dyke was followed by a sequence of smaller intrusions that began in September 1976 and occurred in irregular sequences until 1984<sup>29,39</sup> (Fig. 2). Until 1980, most of the dykes propagated laterally in the crust, accompanied by surface fissuring and faulting. The volumes of erupted lavas were only a small fraction of the intruded volumes. Subsequently, eruptive activity increased with six of the final seven dykes breaching the surface and volumes increasing. It is likely that the change in activity reflects a reduction in extensional stresses to a level that did not allow dykes to propagate over long distances<sup>39</sup>.

Compositional variations in erupted basalts has been documented at Krafla, with more evolved basalts erupting within the Krafla caldera and more primitive ones outside it<sup>40</sup>. This is consistent with a deeper source of primitive magma feeding the shallow magma chamber<sup>41,42</sup>; lateral dyking events emanating from a chemically zoned shallow storage area are one possible explanation for the observed variation in erupted basalt composition<sup>29</sup> with more evolved basalt stored at higher levels being erupted within the caldera. Location of a deep source and its connectivity to the shallow chamber is still a topic of discussion, but deformation and seismicity data rule out models in which primitive basalt rises vertically from the mantle under the entire length of the spreading centre<sup>43</sup>.

A rifting episode began on 6 November 1978 in the Asal-Ghoubbet spreading centre in Djibouti (Afar; Fig. 1). During a two-month swarm, several thousand earthquakes were recorded, the largest with local magnitude 5.3 (ref. 44), and seismicity was observed to propagate to the southeast<sup>44</sup> away from a shallow (2–4 km) magma chamber identified in magnetotelluric data<sup>45</sup>. An extensive set of faults up to 10 km long slipped by up to 0.5 m (ref. 46), and  $16 \times 10^6$  m<sup>3</sup> of basaltic lava was erupted from a 0.75-km-long fissure<sup>44</sup>. Geodetic measurements showed that up to 1.9 m of extension occurred across the rift<sup>46,47</sup>, with a 3-km-wide central graben subsiding by 70 cm and rift flanks uplifting by ~20 cm (ref. 46). The geodetic data have been modelled by the intrusion of two dykes along 20 km of the rift axis with a total thickness of 1.5–3 m in the upper ~5 km of crust<sup>48–50</sup>.

In September 2005, the first subaerial rifting episode in the era of satellite geodesy began in the Dabbahu (northern Manda Hararo) spreading centre, Afar<sup>51–57</sup>. The episode began in earnest on 20 September, with strong seismicity ( $M_w$  3.6–5.6) continuing until 4 October<sup>56</sup>. Earthquakes began at the Dabbahu volcanic complex (DVC) in the north, before jumping to the central Ado ‘Ale volcanic complex (AVC) on 24 September. By 25 September, seismicity was occurring along the entire 60–70 km length of the spreading centre<sup>56</sup>. On 26 September, a small eruption of silicic magma opened

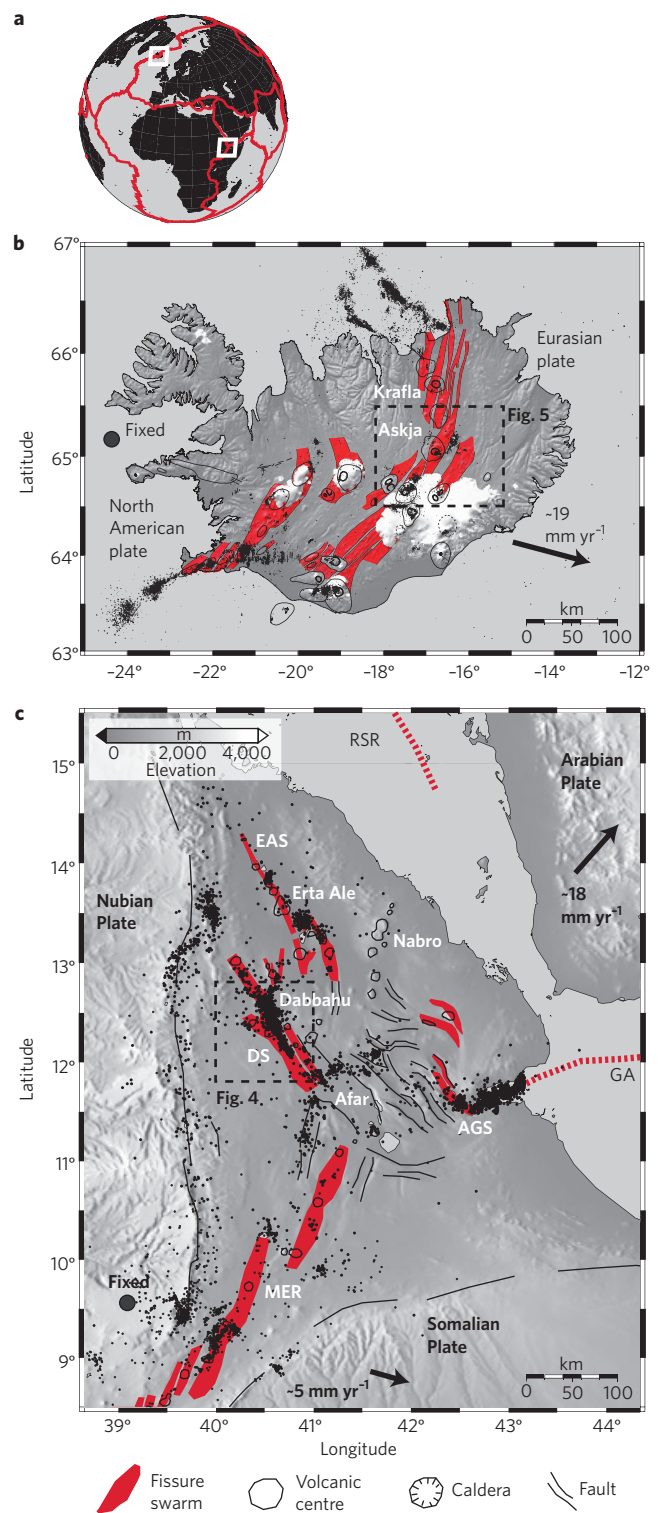


**Figure 1 | Location of subaerial spreading centres.** **a**, Overview map showing plate boundaries. **b**, Tectonic map of Iceland. Extensional faults and fissures form fissure swarms that, together with central volcanoes, form volcanic systems<sup>16</sup>. Earthquakes (black dots) from the South Iceland Lowland (SIL) catalogue of the Icelandic Meteorological Office from 1995 to 2010. Ice caps are indicated (white). **c**, Tectonic map of the Afar region. ‘Magmatic segments’ (from ref. 26) re-plotted in a consistent style with the Icelandic ‘fissure swarms’. Earthquake locations are compiled from temporary networks in Afar<sup>62,64,76,102</sup> and the permanent network in Djibouti<sup>103</sup>. AGS, Asal-Ghoubbet spreading centre; DS, Dabbahu spreading centre; EAS, Erta Ale spreading centre; RSR, Red Sea rift; GA, Gulf of Aden; MER, Main Ethiopian Rift.

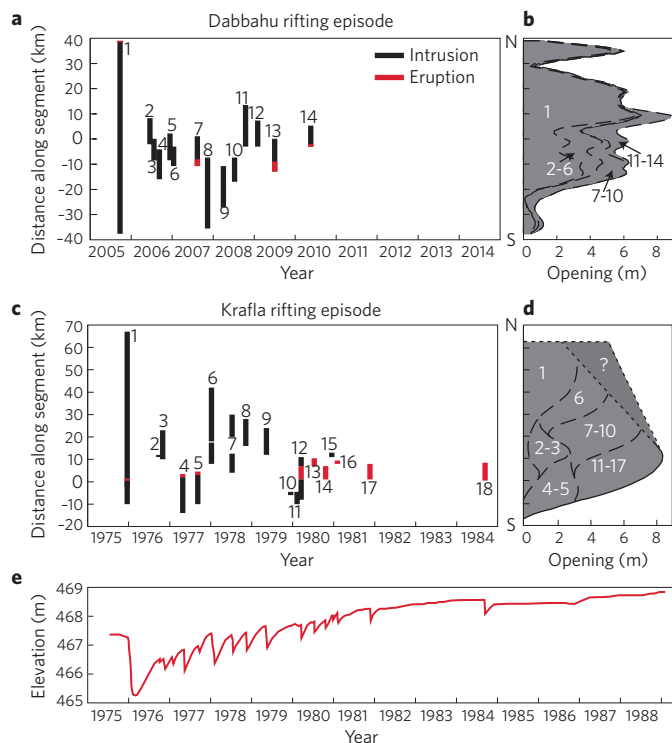


**Figure 2 | Summary of Dabbahu and Krafla rifting episodes.** **a,c**, Location of dyke intrusions (black lines) as a function of time for the Dabbahu rifting episode (**a**; updated from refs 59,65) and Krafla rifting episode (**c**; from refs 29,39). Eruptive fissures in red. Distance is measured from the central feeding zones within the Ado’ Ale Volcanic Complex and Krafla calderas. **(b,d)** Depth-averaged opening during the Dabbahu (**b**) and Krafla (**d**) episodes (updated from refs 33,57,59,65). Opening for Krafla dyke 18 is unavailable but estimated to add about 1 m in the caldera region<sup>39</sup>. **e**, Elevation of the Krafla caldera inferred from tilt observations<sup>29,33</sup>.

a 500-m-long vent between the Dabbahu and Gabho volcanoes in the DVC<sup>51</sup>.

Three-dimensional displacements caused by the initial activity were measured by interferometric synthetic aperture radar (InSAR)<sup>51,52</sup> and sub-pixel offsets in optical satellite images<sup>53,54</sup>. They confirmed that the entire Dabbahu spreading centre was active during this first phase, with near-symmetrical rift-perpendicular opening of up to 8 m. The flanks of the rift uplifted by up to 2 m, with a 2–3-km-wide graben subsiding by 2–3 m at the rift centre. Subsidence of up to 3 m was observed at the DVC under Dabbahu and Gabho. Simple elastic models showed that the deformation was consistent with a large dyke intrusion, up to 10 m thick, in the upper 10 km of crust, with a total volume of 2–2.5 km<sup>3</sup> (refs 51–54). The dyke did not break the surface, but caused faults to slip by up to 3 m on arrays of normal faults above it<sup>58</sup>. The dyke was partially fed from shallow (3–5 km depth) chambers at Dabbahu and Gabho<sup>51,52</sup>, but magma was also probably fed from a deeper source at ~10 km depth within the central AVC (refs 54,56).

Like at Krafla, the initial dyke was followed by a sequence of smaller dyke intrusions, which began in June 2006<sup>59</sup>. So far, there have been 14 dyke intrusions in total, with the most recent occurring in May 2010. These later dykes were typically 2–3 m thick and 10–15 km long, and have a cumulative volume approaching 1 km<sup>3</sup> (refs 59,60). Three dykes broke the surface to produce basaltic fissural eruptions<sup>61</sup>. Seismicity data show that they were all fed from the AVC and propagated at rates of 0.2–0.6 m s<sup>-1</sup> (refs 62–64), comparable to those at Krafla (Fig. 3c,f). Overall, the locations of the dyke intrusions seem to be guided by tectonic driving stress<sup>59,60</sup>,

with the later dykes filling in areas that opened less in the initial dyke (Fig. 2b). However, the location of individual dyke intrusions is also influenced by their immediate predecessor<sup>65</sup>, as seems also to have been the case at Krafla<sup>39</sup>.

In each of these well-observed subaerial rifting episodes, dykes have propagated laterally for many kilometres in the upper crust from a source near the centre of the rift segment. More than one source fed dykes at both Krafla and Dabbahu — at Dabbahu, at least three magma chambers at different locations and depths were involved in the initial phase of activity. At Krafla and Dabbahu, a sequence of small dykes, analogous to earthquake aftershocks, followed the initial main dyke. The overall pattern of dyke opening is likely to be guided by tectonic extensional stresses — these episodes relieve stresses built up during the long periods between episodes. Although intense seismic swarms are associated with rifting episodes, the seismic moment release is small compared with the geodetic moment of the events<sup>62,64</sup>. Deformation is therefore mostly aseismic, due to magma injection.

### Readjustment following rifting episodes

The rifting episodes at Krafla, Asal and Dabbahu have provided opportunities for measuring the Earth’s response to the major stress change associated with rifting. Their geodetic moments are comparable to *M<sub>w</sub>* 7–8 earthquakes, thus producing similar stress changes. A ‘post-rifting’ deformation response due to viscoelastic relaxation is therefore anticipated for several years or decades, with rates (several cm yr<sup>-1</sup>) and length scales (tens of km) comparable to those observed after major earthquakes<sup>66</sup>. In principle, these rifting episodes allow us to determine the rheological properties (elasticity and viscosity) of the crust and mantle that respond to the episode. In practice, separating the response of the magmatic plumbing system from the mechanical viscoelastic relaxation remains problematic.

Measurements of the post-rifting deformation at Krafla come from a GPS network installed in 1987, three years after the rifting episode ended. When these sites were reoccupied in 1990, they revealed spreading rates across the plate boundary of up to 6 cm yr<sup>-1</sup>, around three times higher than the long-term, far-field average<sup>67</sup>. Average rates, at distances of 50 km and more, had in the 1993–2004 period returned to approximately background levels<sup>68</sup>. The deformation data have been modelled using a variety of simple viscous<sup>67,69</sup> or viscoelastic<sup>70,71</sup> rheologies, with no magma movement. These models suggest that viscous relaxation occurs under an elastic upper layer that is ~10 km thick, and that the viscosity of the layer that relaxes fastest is in the range of 1–3 × 10<sup>18</sup> Pas (refs 70,71). Alternatively, magmatic processes in an elastic Earth model have been invoked to explain a 50-km-wide post-rifting deformation signal, with up to ~10 mm yr<sup>-1</sup> uplift in 1993–1998 observed by InSAR<sup>72</sup>.

A long-lived post-rifting deformation transient was also observed after the 1978 Asal rifting episode<sup>73</sup>. Here, a geodetic network has been measured regularly since 1978, initially using trilateration<sup>74</sup> and more recently with GPS<sup>75</sup>. An apparent sharp change in extension rate along a ~5 km baseline spanning the rift, from ~65 mm yr<sup>-1</sup> (1978–1985) to ~17 mm yr<sup>-1</sup> (1985–2003), has been attributed to a sudden change in the rate of magmatic input beneath the rift axis<sup>73</sup>. However, it has also been modelled as a more gradual change of the kind expected from viscoelastic relaxation<sup>75</sup>.

The ongoing Dabbahu rifting episode offers perhaps the best opportunity so far to quantify the response of the viscoelastic and magmatic systems to the stress changes induced by large dyke intrusion. Seismometers were installed around the rift in October 2005<sup>76</sup>, and GPS observations began in January 2006<sup>77</sup>, supplementing regular InSAR acquisitions<sup>54,59,78</sup>. The geodetic data reveal that the post-rifting response began immediately following the initial dyke intrusion. Baselines of 30 km spanning the rift extended at rates as high as 200 mm yr<sup>-1</sup> (> 10 times the plate spreading rate) during the first few years, even after correcting for the effect of shallow dyke

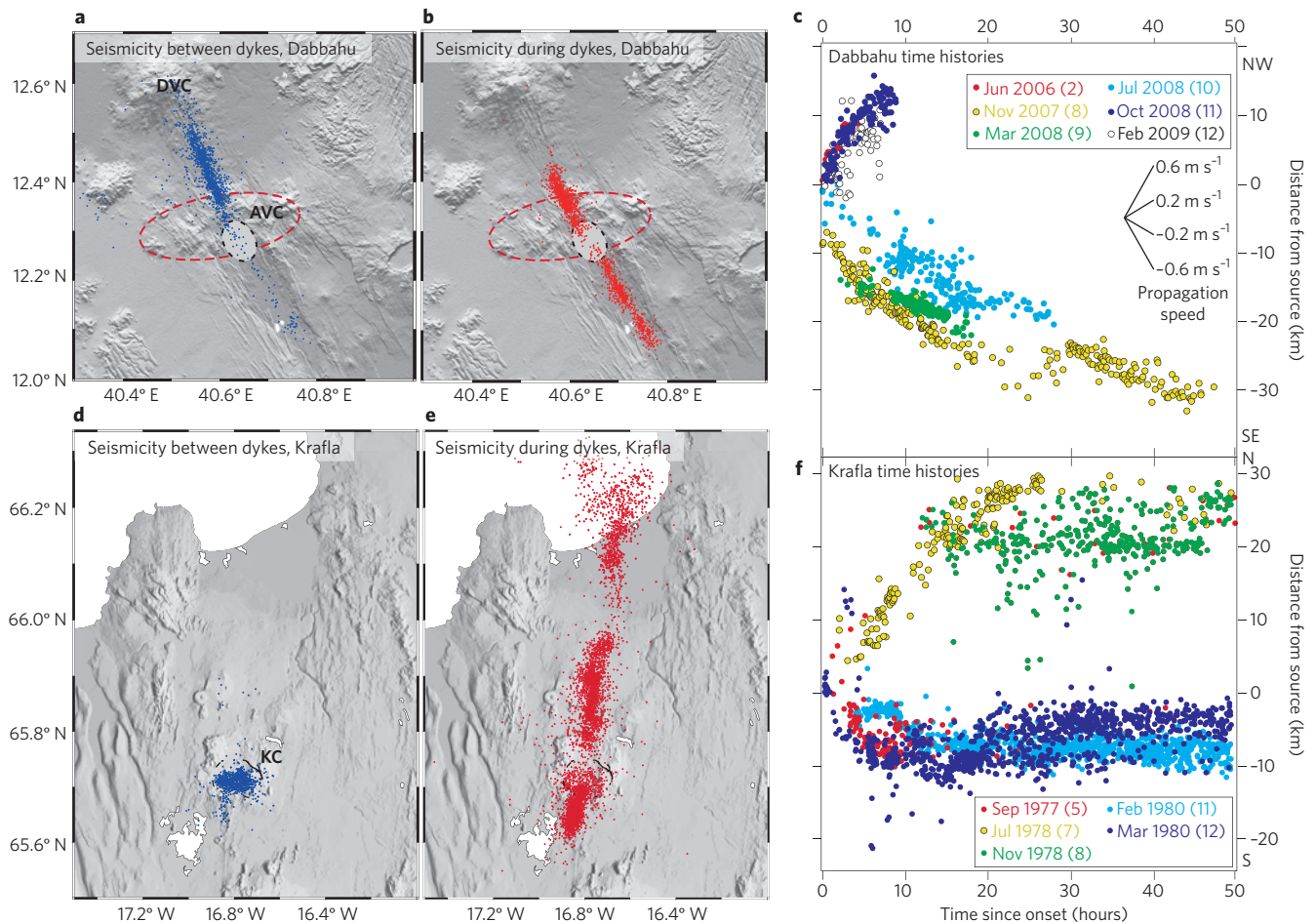


**Figure 3 | Temporal history of dyke intrusions.** **a,d**, Seismicity during intervals between dyke intrusions at Dabbahu<sup>62,76</sup> and Krafla<sup>30,31</sup>. **b,e**, Seismicity associated with dyke intrusions at Dabbahu and Krafla. **c,f**, Temporal progression of seismicity for selected dykes at Dabbahu and Krafla. Dykes colour-coded according to date; dyke numbers (from Fig. 2) in brackets. Data from Dabbahu re-plotted from refs 62,64. Krafla seismicity data from refs 30,31 and previously unpublished records. Seismic data for the two largest earthquake swarms at Krafla have only been partly analysed, leading to apparent seismicity gaps in the northern part of the fissure swarm. Depth cross-section for Dabbahu seismicity in Supplementary Fig. S1. DVC, Dabbahu Volcanic Centre; AVC, Ado 'Ale Volcanic Complex; KC, Krafla Caldera.

intrusions following the large initial event (Fig. 4a). Nooner *et al.*<sup>77</sup> are able to explain the horizontal deformation at GPS sites well by invoking viscoelastic relaxation below a 12–15 km elastic lid, finding a best-fit viscosity of  $4.5\text{--}6.0 \times 10^{18}$  Pas for the relaxing region, slightly higher, but the same order of magnitude as those inferred at Krafla. However, their model cannot explain the observed uplift pattern seen in the InSAR data<sup>79</sup> (Fig. 4b). Deformation around areas of magma supply, notably the AVC at the segment centre, is also not predicted by simple viscoelastic relaxation models — the post-intrusion response is largest near the AVC (Fig. 4a,b), where seismicity data suggest magma replenishment<sup>62</sup>. Opening in the 2005 dyke, which would drive any relaxation, was higher further north (Fig. 2b). Subsidence to the southeast of the spreading centre (SESB, Fig. 4b,c) is also difficult to explain without invoking magma withdrawal, and suggests significant lateral flow of melt in the lower crust. Grandin *et al.*<sup>78</sup> explain the observed InSAR time series using a set of magmatic sources in an elastic half space. By varying the time histories of the strengths of these sources, they are able to produce a good fit to the observations. However, their model includes a deep inflation source in a region of the segment centre where viscoelastic processes might be expected to dominate. The data from Dabbahu suggest that viscoelastic and magmatic processes are both occurring.

One problem that remains to be resolved is that any time-varying pattern of spatial deformation associated with a magmatic system

can be modelled by varying pressure in magma sources embedded in elastic Earth models, as demonstrated in some models for the response to the Krafla, Asal and Dabbahu episodes<sup>72,73,78</sup>. However, for such interpretations to be robust and self-consistent, they must also take into account the viscoelastic relaxation from stresses induced by dyke opening and/or changes to the pressure or volume of subsurface magma chambers. These secondary displacements are often of comparable magnitude to the initial elastic displacements, but develop with a specific predictable spatial and temporal dependence<sup>11</sup>. We therefore advocate the development of models that incorporate contributions from both viscoelastic and magmatic processes. These can only be validated against long time series of observational data, which should capture the transition from magmatic to viscoelastic response. Furthermore, many physical models of spreading ridges call for large variation in structure close to the ridge axis<sup>80</sup>, whereas 'geodetic models' typically only contain horizontal boundaries. Constraining the numerous free parameters in such models requires long periods of geodetic observation and ancillary data on crustal and magmatic properties, for example from seismic and magnetotelluric imaging, repeated microgravity surveys, and petrological studies.

#### Activity between and preceding major episodes

The time-averaged extension rate across a spreading centre cannot exceed the long-term spreading rate. To satisfy this constraint,

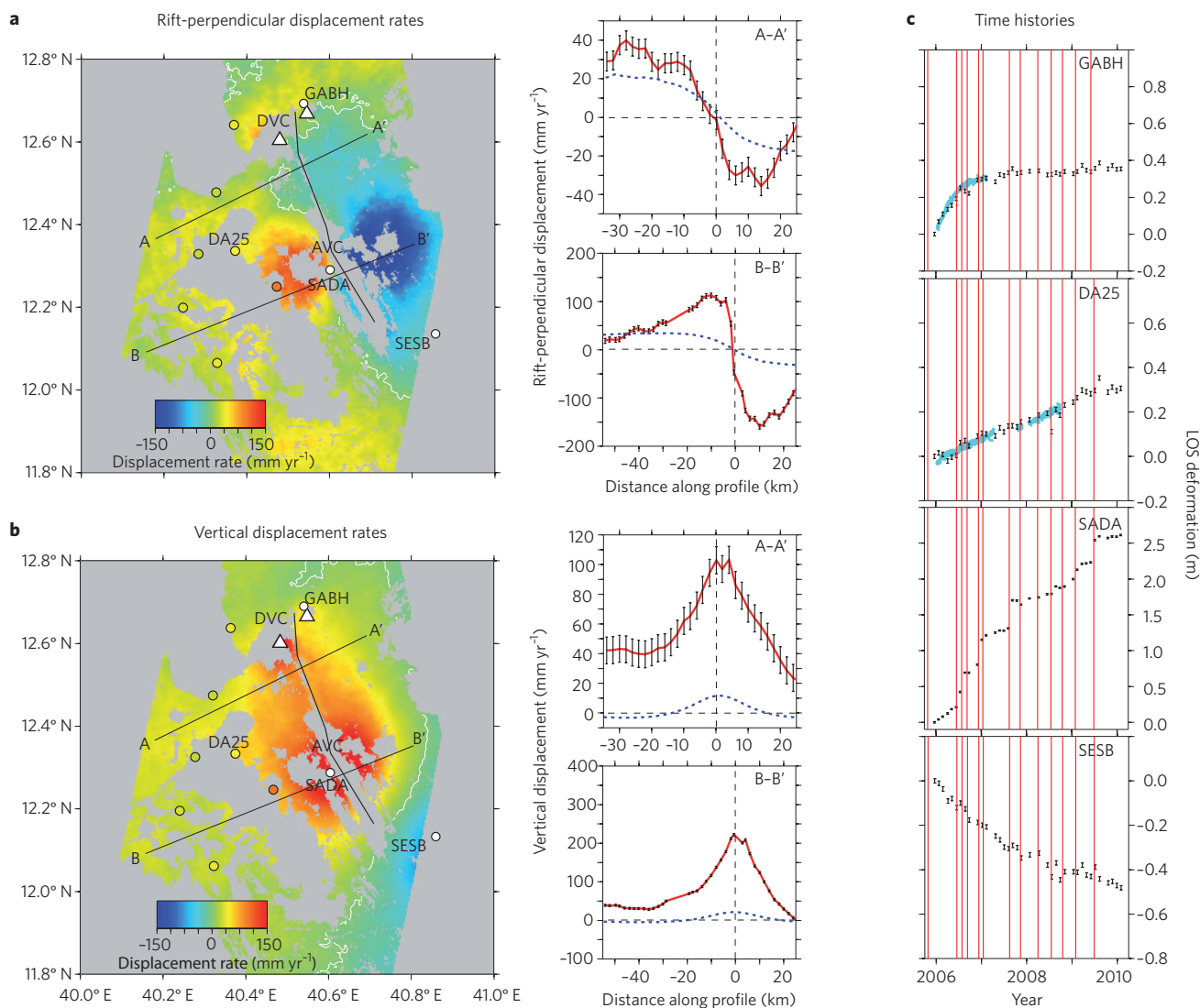


**Figure 4 | Deformation at Dabbahu following the initial dyke intrusion. a, b**, Average rift-perpendicular and vertical displacement rates (June 2006 to January 2010) calculated from ascending and descending interferogram time series and continuous GPS data. Displacements due to dyking have been removed (methods in Supplementary Information and ref. 79). Rift-perpendicular displacements are positive in direction S65° W, perpendicular to the average trend of the rift axis. Displacements at GPS sites (dots) and selected profiles through the geodetic data (red lines with error bars denoting one standard deviation) are shown on the right panel. Displacement rates (blue dashed lines) were calculated using the viscoelastic model parameters of Nooner *et al.*<sup>77</sup>, which best fit the horizontal GPS data alone. DVC, Dabbahu Volcanic Centre; AVC, Ado 'Ale Volcanic Complex. **c**, Time histories of InSAR line-of-sight (LOS) displacement for selected points (locations in **a, b**), including steps during dyke intrusions (red lines). Black error bars denote one standard deviation. Continuous GPS data (cyan) are projected into the LOS. Decreases in LOS displacement are consistent with subsidence and/or eastward motion in ascending track 300 (Envisat beam mode I2; incidence angle -23°). Four-character codes (GABH, DA25, SADA and SESB) indicate the locations of GPS points and/or InSAR time histories.

spreading centres must be relatively quiet for several hundred years between episodes. The geologic and historic record in Iceland broadly satisfies this<sup>16</sup>. Nevertheless, the deformation and seismicity occurring in these long repose periods can offer important constraints on the magmatic systems. Furthermore, evidence from Krafla and Dabbahu suggests that rifting episodes may have significant precursory activity that could be used to provide warnings.

The Askja spreading centre in Iceland's northern volcanic zone (Fig. 1) has the best characterized deformation and seismicity for a spreading centre in this 'inter-rifting' phase of the deformation cycle. Although eruptions occurred in Askja between 1921 and 1929 and in 1961, the most recent episode of major rifting occurred in 1874–1876<sup>81</sup>. Current deformation at Askja has been well documented by GPS, InSAR and levelling data<sup>82–86</sup>, and seismicity has been mapped

using a dense local network<sup>80,87,88</sup>. The zones of horizontal and vertical strain accumulation seem to act on different length scales: extension, at the expected full plate-spreading rate, is distributed over a zone ~80 km wide, whereas rift-axis subsidence is concentrated within the central ~20-km-wide zone of faulting and fissures (Fig. 5). The width of extension is narrower than predicted by simple viscous models<sup>69</sup> but can be explained by simple amagmatic mechanical stretching of a crust in which the elastic layer is thinned near the ridge axis<sup>83</sup>. It is likely that rifting cycle models with spatially variable viscosity structures could also explain the geodetic observations.

Despite the lack of recent magmatic activity, the Askja caldera itself has been subsiding since at least 1983, initially at about 5 cm yr<sup>-1</sup>, and more recently at a rate of ~3 cm yr<sup>-1</sup> (refs 84,85; Fig. 5). Measurements from 1966 to 1971 showed two years of uplift

that was preceded by subsidence. The subsidence can be modelled by a pressure decrease in a shallow magma chamber at 2–3 km depth<sup>82,86</sup>. In the absence of shallow intrusions or eruptive activity, this would require magma to flow out of the shallow chamber to deeper levels<sup>16,82</sup>. A mass decrease inferred from repeated micro-gravity surveys supports this model<sup>89</sup>. Alternatively, local variations in crustal strength or viscoelastic relaxation of hot material beneath the magma chamber might cause the subsidence, without the requirement for significant magma movement<sup>85</sup>.

Recent deployments of dense seismic arrays around Askja have detected several clusters of micro-earthquake activity in the lower crust, which is normally ductile<sup>87,88</sup>. These have been interpreted as areas where high rates of melt movement generate strain rates that are sufficient to cause brittle failure. The spatial distribution of seismicity was persistent over several years, suggesting that melt batches are being channelled upwards through a network of veins and cracks, both within the main areas of volcanic production, but also between them (Fig. 5). The melt seems to stall and accumulate below 10 km depth, well within the ductile part of the crust, forming sills that may crystallize to build the lower crust<sup>88</sup>. This supports geochemical evidence from Iceland and mid-ocean ridges that melt is supplied at multiple injection points<sup>90,91</sup>. The mechanisms and pathways for channelling the deep melt into the focused shallow magmatic centres evident in the geological and geodetic data remain unclear.

Despite the lack of detailed ground-based monitoring, significant precursory activity was observed before the Dabbahu and Krafla rifting episodes. At Krafla, persistent and unusual seismic activity within the caldera was recorded since the installation of permanent stations in 1974, but it is uncertain when it began<sup>29</sup>. At Dabbahu, temporally sparse InSAR observations show that the Gabho volcano began to uplift after September 2001, and that this continued through to the main dyke intrusion<sup>51</sup>. Analysis of regional seismic data<sup>56</sup> showed that intermittent seismicity began in the vicinity of Gabho in April 2005, and that this increased in strength from early September until the main rifting episode began on around 20 September 2005. In both cases, it seems that renewed magma influx to a shallow chamber was the trigger for the start of the rifting episode. In the case of Dabbahu, most of the magma that fed the dyke intrusions was probably present in the shallow system — no precursory uplift was observed at Dabbahu and Ado 'Ale, and the co-dyking subsidence at Gabho exceeded the uplift by a factor of at least 10.

The majority of inter-rifting deformation is likely to be fairly steady and the result of mechanical stretching due to steady far-field plate motions as well as cumulative relaxation from previous episodes. However, this is modulated by pulses of magma recharge to the shallow plumbing system. If well monitored using seismic and geodetic methods, these pulses of recharge offer the potential to predict the onset of future rifting episodes.

### Conceptual model and implications for submerged ridges

Several key lessons can be learned from observations of dynamic processes at subaerial spreading centres that have direct implications for how oceanic crust is created at slow-spreading mid-ocean ridges. Firstly, we emphasize how crustal growth at spreading centres is highly episodic. They can lie dormant for centuries before bursting into life for a short period of time during a rifting episode. The rifting episodes themselves involve the interplay between magma supply and extensional tectonic stresses<sup>39,92</sup>. If magma supply was unlimited, we would expect a single dyke intrusion to relieve the majority of extensional stress in its vicinity; its intruded thickness would then approximately equal the long-term spreading rate multiplied by the repose period. Observations from Dabbahu and Krafla suggest that insufficient magma may be present in the shallow storage systems that feed the dykes — multiple dyke intrusions occur over an extended period of time, guided by and gradually relieving the tectonic stresses. Major eruptions can only occur if the amount of magma supplied to the

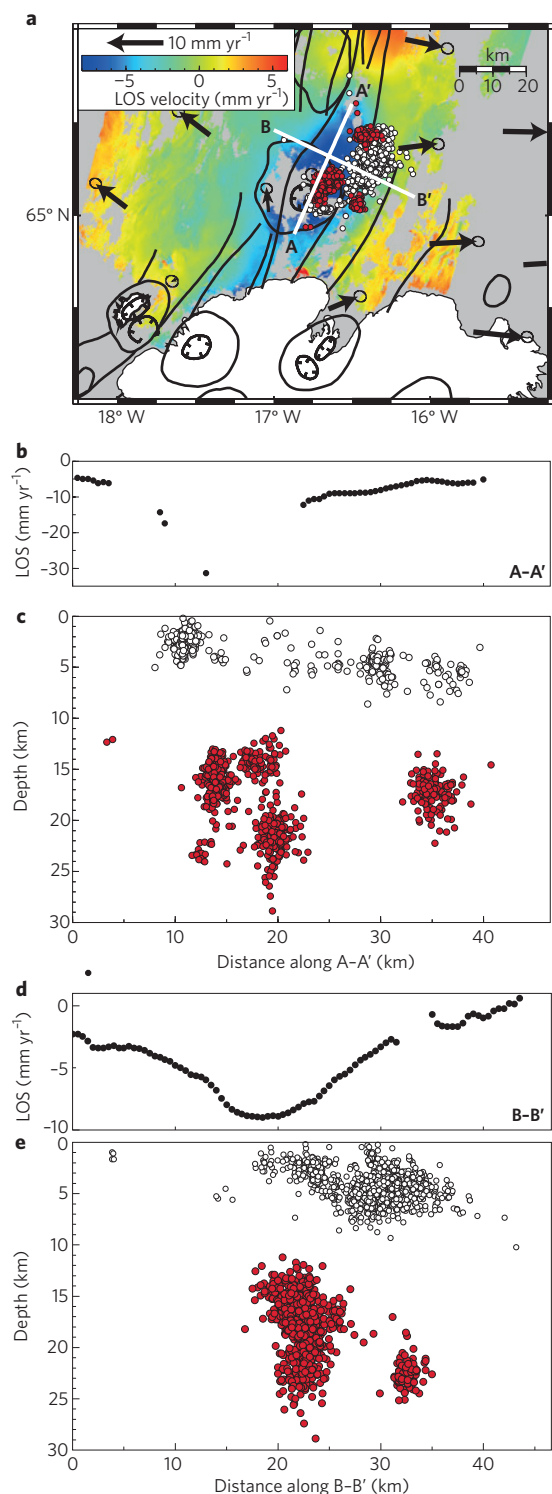


**Figure 5** | Inter-rifting deformation and seismicity at Askja, Iceland. **a**, Map view of deformation and seismicity. Unwrapped line-of-sight displacements (negative values indicate motion away from the satellite) from reprocessed 1993–1998 interferogram<sup>83</sup>. A linear phase ramp has been removed to minimize the contribution of long-wavelength horizontal motions. The remaining signal is mostly subsidence focused on the Askja fissure swarm. GPS displacements during the interval 1993–2004<sup>68</sup> in a plate-boundary reference frame (black vectors). Seismicity<sup>87,88</sup> in brittle upper crust (white dots) and normally aseismic lower crust (red dots). **b,d**, Cross-sections through the LOS velocities, along profiles A–A' (**b**) and B–B' (**d**). **c,e**, Cross-sections showing the depth of the earthquakes along the same profiles.

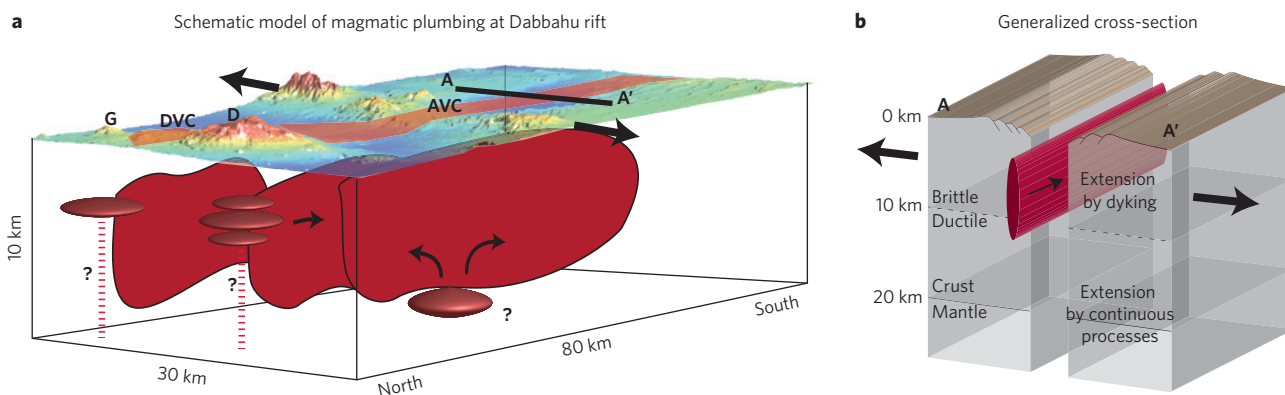


**Figure 6 | Conceptual model for slow-spreading ridges based on observations at subaerial spreading centres. a**, Three-dimensional perspective of upper crust based on current understanding of the Dabbahu rift segment showing probable locations of magma chambers (dark red ellipsoids). Chamber geometries are poorly resolved at present, except at Dabbahu (D), where stacked sills are likely<sup>93</sup>. Dykes are shown as red vertical planes. Topographic data are from the Shuttle Radar Topographic Mission at the zone of fissuring and faulting (highlighted in light red). Inferred hydraulic connections to deeper magma sources (red dashed lines). G, Gabho; DVC, Dabbahu Volcanic Centre; AVC, Ado 'Ale Volcanic Centre. **b**, Cross-section through typical slice of crust away from a magmatic centre. Dyke shown in red. Thin black arrows show magma flow direction; thick arrows show crustal extension direction.

shallow system exceeds that necessary to relieve the extensional stress accumulated in the crust.

Another key result is that multiple crustal magma chambers feed rifting episodes. These can be separated horizontally, as was the case for Dabbahu, where at least three large crustal chambers fed the initial dyke intrusion. Furthermore, vertical separation of discrete magma sources is also likely to be a common feature for plumbing systems. At Krafla, a deep magma source is required as well as the shallow magma chamber to satisfy geodetic and geochemical observations. Although the dykes are fed primarily from a few discrete chambers in the upper to mid-crust, there is good evidence from observations of inter-rifting seismicity at Askja, and geochemistry, that melt is channelled through the lower crust at multiple injection points. The details of the pathways that channel the melt from multiple supply points in the lower crust to a few chambers in the mid to upper crust remain unclear, but are likely to involve channelled flow of melt in the lower crust. Subsidence observed to the south-east of the Dabbahu spreading centre could be evidence for this lower crustal flow.

Our conceptual model for a spreading centre at a slow-spreading ridge (Fig. 6), based on all these observations, consists of a brittle upper crust above a ductile lower crust and mantle. In the upper crust, extension is accommodated primarily by episodic dyking, along with a zone of faulting above the dykes in the top few kilometres. Dykes and faults release elastic strain that has accumulated in the period between rifting episodes. Magma propagates laterally within the dykes from one or more magma chambers, located at different depths; multiple magma chambers, separated by large distances, can be involved in single episodes of injection. The geometry of the crustal magma chambers is in general poorly known — a recent integrated analysis of InSAR, petrology and seismicity data at the Dabbahu volcano concludes that magma is likely to be stored in a series of vertically stacked sills<sup>93</sup>, but further work is required to resolve the geometries of other magma storage systems. The crustal magma chambers are replenished rapidly after magma withdrawal; exponentially decaying uplift above Gabho and Dabbahu (GABH, Fig. 4c) and between dyking events in Krafla (Fig. 2e) suggests a hydraulic connection to a deeper reservoir. The rates of replenishment are low ( $\sim 2 \text{ m}^3 \text{ s}^{-1}$  at Dabbahu and Gabho, and similar at Krafla), implying that the connecting pathways are narrow: feeder conduits with a radius no more than a few metres or, more likely, dykes with comparable cross-sectional areas, are required<sup>94</sup>. In the ductile lower crust, which is rich in partial melt<sup>25</sup>, extension is accommodated continuously by a combination of magmatic addition and viscous flow. Magma can flow

laterally and vertically within the ductile region, causing earthquakes where the strain rates are high. Time-dependent viscous flow is most rapid immediately following a rifting episode. Although this model is somewhat specific to Dabbahu, it only requires minor modification to apply to other spreading centres.

Of course, caution is required before directly ascribing the phenomenology of a few subaerial spreading centres to all slow-spreading ridges. The subaerial centres are by their very nature anomalous, in particular because of their thick crust and the influence of mantle plumes. Furthermore, interaction with ice loads plays a significant role in the observed processes on Iceland<sup>95,96</sup> and we might expect hydrothermal activity to be more vigorous at submerged ridges. Nevertheless, it is likely that considerable time will pass before we are able to make direct observations of the processes occurring on submerged spreading centres with the temporal and spatial resolution that is possible on land.

### Unresolved issues

Several issues remain that should be the focus of research in the coming years. A key unsolved question is what controls the variability in style of magma plumbing at spreading centres. For example, recent analysis of geodetic data from an eruption in November 2008 suggests that an elongated axial magma chamber, similar to those found at fast-spreading ridges, exists in the Erta Ale spreading centre<sup>97</sup> (Afar; Fig. 1), north of the famous lava lake<sup>98</sup>. At submerged ridges, spreading rate and magma supply are primary controls on style of magma plumbing<sup>99</sup>. Further work is required to determine whether these same factors control the morphology of subaerial ridges.

Observations from subaerial rifting episodes show that interactions can occur between multiple magmatic centres during a single episode and that the driving tectonic stresses play a key role in guiding dyke intrusions. Entire spreading centres may interact on a longer timescale — geological evidence suggests that the Krafla spreading centre had only one eruptive episode from 8,000–3,000 years BP (ref. 100), whereas activity on a neighbouring spreading centre increased. Further research is required into the spatial and temporal scale of such interactions between segments. We also encourage the further development of ocean-bottom geodetic and seismic instruments to capture dynamic processes occurring on submerged mid-ocean ridges.

In summary, geophysical observations at subaerial spreading centres enable us to build a picture of their dynamic internal mechanics.

We have shown that magma moves through plumbing systems that can be quite complex. Multiple magma storage systems seem able to interact and feed laterally propagating dykes during rifting episodes, which can last several years. Large-volume eruptions are possible at slow-spreading centres — for example, more than 10 km<sup>3</sup> of lava was erupted from Laki (Iceland) over 8 months in 1783–1784<sup>101</sup>. Before we can make progress in forecasting these large eruptions, rifting-cycle models will need to fully incorporate realistic crust and mantle properties, as well as the dynamic transport of magma. Long-term interdisciplinary observations of subaerial and submerged spreading centres are required to develop and test such models.

## References

- Toomey, D. R., Jousset, D., Dunn, R. A., Wilcock, W. S. D. & Detrick, R. S. Skew of mantle upwelling beneath the East Pacific Rise governs segmentation. *Nature* **446**, 409–414 (2007).
- Dunn, R. A. & Toomey, D. R. Seismological evidence for three-dimensional melt migration beneath the east Pacific rise. *Nature* **388**, 259–262 (1997).
- Singh, S. C. *et al.* Discovery of a magma chamber and faults beneath a mid-Atlantic Ridge hydrothermal field. *Nature* **442**, 1029–1032 (2006).
- Smith, D. K. & Cann, J. R. Constructing the upper crust of the mid-Atlantic Ridge: a reinterpretation based on the Puna Ridge, Kilauea Volcano. *J. Geophys. Res.-Sol. Earth* **104**, 25379–25399 (1999).
- Canales, J. P., Nedimovic, M. R., Kent, G. M., Carbotte, S. M. & Detrick, R. S. Seismic reflection images of a near-axis melt sill within the lower crust at the Juan de Fuca ridge. *Nature* **460**, 89–93 (2009).
- Dzurisin, D. *Volcano Deformation* (Springer Praxis, 2006).
- Poland, M., Hamburger, M. & Newman, A. The changing shapes of active volcanoes: history, evolution, and future challenges for volcano geodesy. *J. Volcanol. Geoth. Res.* **150**, 1–13 (2006).
- Chouet, B. Volcano seismology. *Pure Appl. Geophys.* **160**, 739–788 (2003).
- McNutt, S. R. Volcanic seismology. *Annu. Rev. Earth Planet. Sci.* **33**, 461–491 (2005).
- Perfit, M. R. & Chadwick, W. W. Jr in *Faulting and Magmatism at Mid-ocean Ridges* (ed. Buck, R. W. *et al.*) **106**, 59–116 (Geophysical Monograph Series, 1998).
- Nooner, S. L. & Chadwick, W. W. Volcanic inflation measured in the caldera of Axial Seamount: Implications for magma supply and future eruptions. *Geochem. Geophys. Geosys.* **10**, Q02002 (2009).
- Tolstoy, M. *et al.* A sea-floor spreading event captured by seismometers. *Science* **314**, 1920–1922 (2006).
- Delaney, J. R. *et al.* The quantum event of oceanic crustal accretion: Impacts of diking at mid-ocean ridges. *Science* **281**, 222–230 (1998).
- Sinton, J. *et al.* Volcanic eruptions on mid-ocean ridges: New evidence from the superfast spreading East Pacific Rise, 17°–19° S. *J. Geophys. Res.-Sol. Earth* **107**, 2115 (2002).
- Demets, C., Gordon, R. G., Argus, D. F. & Stein, S. Current plate motions. *Geophys. J. Int.* **101**, 425–478 (1990).
- Sigmundsson, F. *Iceland Geodynamics: Crustal Deformation and Divergent Plate Tectonics* (Springer, 2006).
- Bastow, I. D. & Keir, D. The protracted development of the continent-ocean transition in Afar. *Nature Geosci.* **4**, 248–250 (2011).
- Wolfenden, E., Ebinger, C., Yirgu, G., Renne, P. R. & Kelley, S. P. Evolution of a volcanic rifted margin: Southern Red Sea, Ethiopia. *Geol. Soc. Am. Bull.* **117**, 846–864 (2005).
- ArRajehi, A. *et al.* Geodetic constraints on present-day motion of the Arabian Plate: Implications for Red Sea and Gulf of Aden rifting. *Tectonics* **29**, Tc3011 (2010).
- McClusky, S. *et al.* Kinematics of the southern Red Sea-Afar Triple Junction and implications for plate dynamics. *Geophys. Res. Lett.* **37**, L05301 (2010).
- Hill, R. I., Campbell, I. H., Davies, G. F. & Griffiths, R. W. Mantle plumes and continental tectonics. *Science* **256**, 186–193 (1992).
- Darbyshire, F. A., White, R. S. & Priestley, K. F. Structure of the crust and uppermost mantle of Iceland from a combined seismic and gravity study. *Earth Planet. Sci. Lett.* **181**, 409–428 (2000).
- Furman, T. *et al.* Heads and tails: 30 million years of the Afar plume. *Geol. Soc. London Spec. Publ.* **259**, 97–121 (2006).
- Poore, H., White, N. & MacLennan, J. Ocean circulation and mantle melting controlled by radial flow of hot pulses in the Iceland plume. *Nature Geosci.* **4**, 558–561 (2011).
- Hammond, J. *et al.* The nature of the crust beneath the Afar triple junction: evidence from receiver functions. *Geochem. Geophys. Geosys.* **12**, Q12004 (2011).
- Hayward, N. J. & Ebinger, C. J. Variations in the along-axis segmentation of the Afar Rift system. *Tectonics* **15**, 244–257 (1996).
- Tucholke, B. E. & Lin, J. A geological model for the structure of ridge segments in slow-spreading ocean crust. *J. Geophys. Res.-Sol. Earth* **99**, 11937–11958 (1994).
- Bjornsson, A., Saemundsson, K., Einarsson, P., Tryggvason, E. & Gronvold, K. Current rifting episode in north Iceland. *Nature* **266**, 318–323 (1977).
- Einarsson, P. The volcanic unrest at Krafla 1975–1989. *Náttúra Mývatn* 96–139 (Hið íslenska náttúrufræðifélag, 1991).
- Brandsdóttir, B. & Einarsson, P. Seismic activity associated with the September 1977 deflation of the Krafla central volcano in northeastern Iceland. *J. Volcanol. Geotherm. Res.* **6**, 197–212 (1979).
- Einarsson, P. & Brandsdóttir, B. Seismological evidence for lateral magma intrusion during the July 1978 deflation of the Krafla Volcano in NE Iceland. *J. Geophys.-Z. Geophys.* **47**, 160–165 (1980).
- Opheim, J. A. & Gudmundsson, A. Formation and geometry of fractures, and related volcanism, of the Krafla fissure swarm, northeast Iceland. *Geol. Soc. Am. Bull.* **101**, 1608–1622 (1989).
- Tryggvason, E. Widening of the Krafla fissure swarm during the 1975–1981 volcano-tectonic episode. *Bull. Volcanol.* **47**, 47–69 (1984).
- Bjornsson, A. Dynamics of crustal rifting in NE Iceland. *J. Geophys. Res.-Solid* **90**, 151–162 (1985).
- Bjornsson, A., Johnsen, G., Sigurdsson, S., Thorbergsson, G. & Tryggvason, E. Rifting of the plate boundary in north Iceland 1975–1978. *J. Geophys. Res.* **84**, 3029–3038 (1979).
- Brandsdóttir, B., Menke, W., Einarsson, P., White, R. S. & Staples, R. K. Faroe-Iceland ridge experiment 2: crustal structure of the Krafla central volcano. *J. Geophys. Res.-Sol. Earth* **102**, 7867–7886 (1997).
- Einarsson, P. S-wave shadows in the Krafla caldera in NE-Iceland, evidence for a magma chamber in the crust. *Bull. Volcanol.* **41**, 187–195 (1978).
- Brandsdóttir, B. & Menke, W. H. Thin low-velocity zone within the Krafla caldera, NE-Iceland attributed to a small magma chamber. *Geophys. Res. Lett.* **19**, 2381–2384 (1992).
- Buck, W. R., Einarsson, P. & Brandsdóttir, B. Tectonic stress and magma chamber size as controls on dike propagation: Constraints from the 1975–1984 Krafla rifting episode. *J. Geophys. Res.-Sol. Earth* **111**, B12404 (2006).
- Gronvold, K. in *Eos Trans. AGU Fall Meet. Suppl.* **87**(52), abstr. T33E-08 (2006).
- Tryggvason, E. Multiple magma reservoirs in a rift-zone volcano — ground deformation and magma transport during the September 1984 eruption of Krafla, Iceland. *J. Volcanol. Geother. Res.* **28**, 1–44 (1986).
- Arnadóttir, T., Sigmundsson, F. & Delaney, P. T. Sources of crustal deformation associated with the Krafla, Iceland, eruption of September 1984. *Geophys. Res. Lett.* **25**, 1043–1046 (1998).
- Gudmundsson, A. Infrastructure and mechanics of volcanic systems in Iceland. *J. Volcanol. Geother. Res.* **64**, 1–22 (1995).
- Abdallah, A. *et al.* Relevance of Afar seismicity and volcanism to the mechanics of accreting plate boundaries. *Nature* **282**, 17–23 (1979).
- Ruegg, J. Structure profonde de la croûte et du manteau supérieur du Sud-Est de l'Afar d'après les données sismiques. *Ann. Geophys.* **31**, 329–360 (1975).
- Allard, P., Tazieff, H. & Dajlevic, D. Observations of seafloor spreading in Afar during the November 1978 fissure eruption. *Nature* **279**, 30–33 (1979).
- Ruegg, J. C., Lepine, J. C., Tarantola, A. & Kasser, M. Geodetic measurements of rifting associated with a seismo-volcanic crisis in Afar. *Geophys. Res. Lett.* **6**, 817–820 (1979).
- Tarantola, A., Ruegg, J. C. & Lepine, J. P. Geodetic evidence for rifting in Afar 2: vertical displacements. *Earth Planet. Sci. Lett.* **48**, 363–370 (1980).
- Stein, R. S., Briole, P., Ruegg, J. C., Tapponnier, P. & Gasse, F. Contemporary, Holocene, and Quaternary deformation of the Asal rift, Djibouti — implications for the mechanics of slow spreading ridges. *J. Geophys. Res.-Sol. Earth* **96**, 21789–21806 (1991).
- Rubin, A. M. & Pollard, D. D. Dike-induced faulting in rift zones of Iceland and Afar. *Geology* **16**, 413–417 (1988).
- Wright, T. J. *et al.* Magma-maintained rift segmentation at continental rupture in the 2005 Afar dyking episode. *Nature* **442**, 291–294 (2006).
- Ayele, A. *et al.* The volcano-seismic crisis in Afar, Ethiopia, starting September 2005. *Earth Planet. Sci. Lett.* **255**, 177–187 (2007).
- Barisin, I., Leprince, S., Parsons, B. & Wright, T. Surface displacements in the September 2005 Afar rifting event from satellite image matching: asymmetric uplift and faulting. *Geophys. Res. Lett.* **36**, L07301 (2009).
- Grandin, R. *et al.* September 2005 Manda Hararo-Dabbahu rifting event, Afar (Ethiopia): constraints provided by geodetic data. *J. Geophys. Res.-Sol. Earth* **114**, B08404 (2009).
- Rowland, J. *et al.* Fault growth at a nascent slow-spreading ridge: 2005 Dabbahu rifting episode, Afar. *Geophys. J. Int.* **171**, 1226–1246 (2007).
- Ayele, A. *et al.* September 2005 mega-dike emplacement in the Manda-Hararo nascent oceanic rift (Afar depression). *Geophys. Res. Lett.* **36**, L20306 (2009).
- Ebinger, C. *et al.* Length and timescales of rift faulting and magma intrusion: the Afar rifting cycle from 2005 to present. *Annu. Rev. Earth Planet. Sci.* **38**, 439–466 (2010).

58. Rowland, J. *et al.* Fault growth at a nascent slow spreading ridge: 2005 Dabbahu rifting episode, Afar. *Geophys. J. Int.* **171**, 1226–1246 (2007).
59. Hamling, I. *et al.* Geodetic observations of the ongoing Dabbahu rifting episode: new dyke intrusions in 2006 and 2007. *Geophys. J. Int.* **178**, 989–1003 (2009).
60. Grandin, R. *et al.* Sequence of rifting in Afar, Manda-Hararo rift, Ethiopia, 2005–2009: Time-space evolution and interactions between dikes from interferometric synthetic aperture radar and static stress change modeling. *J. Geophys. Res.-Sol. Earth* **115**, B10413 (2010).
61. Ferguson, D. J. *et al.* Recent rift-related volcanism in Afar, Ethiopia. *Earth Planet. Sci. Lett.* **292**, 409–418 (2010).
62. Belachew, M. *et al.* Comparison of dike intrusions in an incipient seafloor-spreading segment in Afar, Ethiopia: seismicity perspectives. *J. Geophys. Res.-Sol. Earth* **116**, B06405 (2011).
63. Grandin, R. *et al.* Seismicity during lateral dike propagation: insights from new data in the recent Manda Hararo-Dabbahu rifting episode (Afar, Ethiopia). *Geochem. Geophys. Geosys.* **12**, Q0AB08 (2011).
64. Keir, D. *et al.* Evidence for focused magmatic accretion at segment centers from lateral dike injections captured beneath the Red Sea rift in Afar. *Geology* **37**, 59–62 (2009).
65. Hamling, I. J., Wright, T. J., Calais, E., Bennati, L. & Lewi, E. Stress transfer between thirteen successive dyke intrusions in Ethiopia. *Nature Geosci.* **3**, 806–806 (2010).
66. Burgmann, R. & Dresen, G. Rheology of the lower crust and upper mantle: evidence from rock mechanics, geodesy, and field observations. *Ann. Rev. Earth Planet. Sci.* **36**, 531–567 (2008).
67. Foulger, G. R. *et al.* Post-rifting stress-relaxation at the divergent plate boundary in northeast Iceland. *Nature* **358**, 488–490 (1992).
68. Arnadóttir, T. *et al.* Glacial rebound and plate spreading: results from the first countrywide GPS observations in Iceland. *Geophys. J. Int.* **177**, 691–716 (2009).
69. Heki, K., Foulger, G. R., Julian, B. R. & Jahn, C. H. Plate dynamics near divergent boundaries - geophysical implications of crustal deformation in NE Iceland. *J. Geophys. Res.-Sol. Earth* **98**, 14279–14297 (1993).
70. Hofton, M. A. & Foulger, G. R. Post-rifting anelastic deformation around the spreading plate boundary, north Iceland 1: modeling of the 1987–1992 deformation field using a viscoelastic Earth structure. *J. Geophys. Res.-Sol. Earth* **101**, 25403–25421 (1996).
71. Pollitz, F. F. & Sacks, I. S. Viscosity structure beneath northeast Iceland. *J. Geophys. Res.-Sol. Earth* **101**, 17771–17793 (1996).
72. De Zeeuw-van Dalen, E., Pedersen, R., Sigmundsson, F. & Pagli, C. Satellite radar interferometry 1993–1999 suggests deep accumulation of magma near the crust-mantle boundary at the Krafla volcanic system, Iceland. *Geophys. Res. Lett.* **31**, L13611 (2004).
73. Cattin, R. *et al.* Numerical modelling of Quaternary deformation and post-rifting displacement in the Asal-Ghoubbet rift (Djibouti, Africa). *Earth Planet. Sci. Lett.* **239**, 352–367 (2005).
74. Ruegg, J. C. & Kasser, M. Deformation across the Asal-Ghoubbet Rift, Djibouti, uplift and crustal extension 1979–1986. *Geophys. Res. Lett.* **14**, 745–748 (1987).
75. Vigny, C. *et al.* Twenty-five years of geodetic measurements along the Tadjoura-Asal rift system, Djibouti, East Africa. *J. Geophys. Res.-Sol. Earth* **112**, B06410 (2007).
76. Ebinger, C. *et al.* Capturing magma intrusion and faulting processes during continental rupture: seismicity of the Dabbahu (Afar) rift. *Geophys. J. Int.* **174**, 1138–1152 (2008).
77. Nooner, S. *et al.* Post-rifting relaxation in the Afar region, Ethiopia. *Geophys. Res. Lett.* **36**, L21308 (2009).
78. Grandin, R. *et al.* Transient rift opening in response to multiple dike injections in the Manda Hararo rift (Afar, Ethiopia) imaged by time-dependent elastic inversion of interferometric synthetic aperture radar data. *J. Geophys. Res.-Sol. Earth* **115**, B11499 (2010).
79. Hamling, I. J. *Measuring and modelling deformation during the Dabbahu (Afar) rifting episode*. PhD Thesis, Univ. Leeds (2010).
80. Morgan, J. P., Parmentier, E. M. & Lin, J. Mechanisms for the origin of midocean ridge axial topography — implications for the thermal and mechanical structure of accreting plate boundaries. *J. Geophys. Res.-Solid* **92**, 12823–12836 (1987).
81. Sigurdsson, H. & Sparks, R. S. J. Rifting episode in north Iceland in 1874–1875 and the eruptions of Askja and Sveinagja. *Bull. Volcanol.* **41**, 149–167 (1978).
82. Pagli, C., Sigmundsson, F., Arnadóttir, T., Einarsson, P. & Sturkell, E. Deflation of the Askja volcanic system: constraints on the deformation source from combined inversion of satellite radar interferograms and GPS measurements. *J. Volcanol. Geotherm. Res.* **152**, 97–108 (2006).
83. Pedersen, R., Sigmundsson, F. & Masterlark, T. Rheologic controls on inter-rifting deformation of the Northern Volcanic Zone, Iceland. *Earth Planet. Sci. Lett.* **281**, 14–26 (2009).
84. Sturkell, E. *et al.* Volcano, geodesy and magma dynamics in Iceland. *J. Volcanol. Geotherm. Res.* **150**, 14–34 (2006).
85. De Zeeuw-van Dalen, E., Pedersen, R., Hooper, A. & Sigmundsson, F. Subsidence of Askja caldera 2000–2009: modelling of deformation processes at an extensional plate boundary, constrained by time series InSAR analysis. *J. Volcanol. Geotherm. Res.* **213–214**, 72–82 (2012).
86. Sturkell, E., Sigmundsson, F. & Slunga, R. 1983–2003 decaying rate of deflation at Askja caldera: pressure decrease in an extensive magma plumbing system at a spreading plate boundary. *Bull. Volcanol.* **68**, 727–735 (2006).
87. Soosalu, H. *et al.* Lower-crustal earthquakes caused by magma movement beneath Askja volcano on the north Iceland rift. *Bull. Volcanol.* **72**, 55–62 (2010).
88. Key, J., White, R. S., Soosalu, H. & Jakobsdóttir, S. S. Multiple melt injection along a spreading segment at Askja, Iceland. *Geophys. Res. Lett.* **38**, L05301 (2011).
89. De Zeeuw-Van Dalen, E., Rymmer, H., Sigmundsson, F. & Sturkell, E. Net gravity decrease at Askja volcano, Iceland: constraints on processes responsible for continuous caldera deflation, 1988–2003. *J. Volcanol. Geotherm. Res.* **139**, 227–239 (2005).
90. Langmuir, C. H., Bender, J. F. & Batiza, R. Petrological and tectonic segmentation of the East Pacific Rise, 5°30′–14°30′N. *Nature* **322**, 422–429 (1986).
91. MacLennan, J. Concurrent mixing and cooling of melts under Iceland. *J. Petrol.* **49**, 1931–1953 (2008).
92. Qin, R. & Buck, W. R. Why meter-wide dikes at oceanic spreading centers? *Earth and Planetary Science Letters* **265**, 466–474 (2008).
93. Field, L., Blundy, J., Brooker, R. A., Wright, T. J. & Yirgu, G. Magma storage conditions beneath Dabbahu Volcano (Ethiopia) constrained by petrology, seismicity and satellite geodesy. *Bull. Volcanol.* <http://dx.doi.org/10.1007/s00445-012-0580-6> (2012).
94. Turcotte, D. L. & Schubert, G. *Geodynamics* (Cambridge Univ., 2002).
95. Jull, M. & McKenzie, D. The effect of deglaciation on mantle melting beneath Iceland. *J. Geophys. Res.-Sol. Earth* **101**, 21815–21828 (1996).
96. Pagli, C. *et al.* Glacio-isostatic deformation around the Vatnajökull ice cap, Iceland, induced by recent climate warming: GPS observations and finite element modeling. *J. Geophys. Res.-Sol. Earth* **112**, B08405 (2007).
97. Pagli, C. *et al.* Dynamics of an axial magma chamber at the Erta Ale slow spreading segment. *Nature Geosci.* **5**, 284–288 (2012).
98. Oppenheimer, C. & Francis, P. Implications of long-lived lava lakes for geomorphological and plutonic processes at Erta Ale volcano, Afar. *J. Volcanol. Geothermal Research* **80**, 101–111 (1998).
99. Morgan, J. P. & Ghen, Y. J. Dependence of ridge-axis morphology on magma supply and spreading rate. *Nature* **364**, 706–708 (1993).
100. Sæmundsson, K. Geology of the Krafla volcanic system. *Náttúra Mývatns* 26–95 (Hið íslenska náttúrufræðifélag, 1991).
101. Thordarson, T. & Self, S. The Laki (Skaftár-Fires) and Grimsvotn eruptions in 1783–1785. *Bull. Volcanol.* **55**, 233–263 (1993).
102. Keir, D. *et al.* Lower crustal earthquakes near the Ethiopian rift induced by magmatic processes. *Geochem. Geophys. Geosys.* **10**, Q0ab02 (2009).
103. Doube, C. *et al.* Crustal structure and magmato-tectonic processes in an active rift (Asal-Ghoubbet, Afar, East Africa): 2. Insights from the 23-year recording of seismicity since the last rifting event. *J. Geophys. Res.-Sol. Earth* **112**, B05406 (2007).

## Acknowledgments

Our work is supported by NERC grants NE/D008611/1, NE/D01039X/1 and NE/E007414/1, NSF grants EAR-0635789 and EAR-0613651, a NERC-COMET+ studentship to I.J.H., and a Royal Society University Research Fellowship to T.J.W. Authors in Iceland were supported by the Icelandic Research Fund (through Volcano Anatomy project) and the University of Iceland Research Fund. We are grateful to Janet Key and Bob White for providing seismicity data for Askja, and to the numerous scientists involved in the countless field experiments in Afar and Iceland that have collected the data sets described here. The manuscript was improved by thoughtful comments from Bob White and Falk Amelung. The Centre for the Observation and Modelling of Earthquakes, Volcanoes and Tectonics (COMET+) is part of the UK National Environment Research Council's National Centre for Earth Observation.

## Author Contributions

T.J.W. and F.S. planned and wrote the article with input from all other authors. Previously unpublished seismic data from Krafla were collected and analysed by P.E. and B.B. Also, D.K., R.P., B.B. and T.W. constructed Fig. 1; B.B., M.B., C.P. and I.J.H. collated data from Dabbahu and Krafla to build Figs 2 and 3; I.J.H. and T.W. conducted a new analysis of InSAR data to make Fig. 4; R.P. and C.P. created Fig. 5; T.J.W. and F.S. designed Fig. 6 with input from other authors.

## Additional Information

The authors declare no competing financial interests. Supplementary information accompanies this paper on [www.nature.com/naturegeoscience](http://www.nature.com/naturegeoscience). Correspondence and requests for materials should be addressed to T.J.W.